

Contract No:

This document was prepared in conjunction with work accomplished under Contract No. DE-AC09-08SR22470 with the U.S. Department of Energy (DOE) Office of Environmental Management (EM).

Disclaimer:

This work was prepared under an agreement with and funded by the U.S. Government. Neither the U. S. Government or its employees, nor any of its contractors, subcontractors or their employees, makes any express or implied:

- 1) warranty or assumes any legal liability for the accuracy, completeness, or for the use or results of such use of any information, product, or process disclosed; or
- 2) representation that such use or results of such use would not infringe privately owned rights; or
- 3) endorsement or recommendation of any specifically identified commercial product, process, or service.

Any views and opinions of authors expressed in this work do not necessarily state or reflect those of the United States Government, or its contractors, or subcontractors.

We put science to work.™



**Savannah River
National Laboratory™**

OPERATED BY SAVANNAH RIVER NUCLEAR SOLUTIONS

A U.S. DEPARTMENT OF ENERGY NATIONAL LABORATORY • SAVANNAH RIVER SITE • AIKEN, SC

Preliminary Disposal Limits, Plume Interaction Factors, and Final Disposal Limits

G. P. Flach

January 11, 2018

SRNL-STI-2018-00020, Revision 0

SRNL.DOE.GOV

DISCLAIMER

This work was prepared under an agreement with and funded by the U.S. Government. Neither the U.S. Government or its employees, nor any of its contractors, subcontractors or their employees, makes any express or implied:

1. warranty or assumes any legal liability for the accuracy, completeness, or for the use or results of such use of any information, product, or process disclosed; or
2. representation that such use or results of such use would not infringe privately owned rights; or
3. endorsement or recommendation of any specifically identified commercial product, process, or service.

Any views and opinions of authors expressed in this work do not necessarily state or reflect those of the United States Government, or its contractors, or subcontractors.

Printed in the United States of America

**Prepared for
U.S. Department of Energy**

Keywords: *E-Area*
Performance Assessment

Retention: *Permanent*

Preliminary Disposal Limits, Plume Interaction Factors, and Final Disposal Limits

G. P. Flach

January 11, 2018

Prepared for the U.S. Department of Energy under
contract number DE-AC09-08SR22470.



OPERATED BY SAVANNAH RIVER NUCLEAR SOLUTIONS

REVIEWS AND APPROVALS

AUTHORS:

G. P. Flach, Environmental Modeling Date

TECHNICAL REVIEW:

L. L. Hamm, Threat Assessments, Reviewed per E7 2.60 Date

APPROVAL:

D. A. Crowley, Manager Date
Environmental Modeling

L. T. Reid, Manager Date
Environmental Restoration Technologies

EXECUTIVE SUMMARY

In the 2008 E-Area Performance Assessment (PA), each *final disposal limit* was constructed as the product of a *preliminary disposal limit* and a *plume interaction factor*. The following mathematical development demonstrates that performance objectives are generally expected to be satisfied with high confidence under practical PA scenarios using this method. However, radionuclides that experience significant decay between a disposal unit and the 100-meter boundary, such as H-3 and Sr-90, can challenge performance objectives, depending on the disposed-of waste composition, facility geometry, and the significance of the plume interaction factor. Pros and cons of analyzing single disposal units or multiple disposal units as a group in the preliminary disposal limits analysis are also identified.

TABLE OF CONTENTS

LIST OF TABLES	vii
LIST OF FIGURES	vii
LIST OF ABBREVIATIONS.....	viii
1.0 Introduction.....	1
2.0 Preliminary disposal limits	1
3.0 Plume interaction factors	3
4.0 Final disposal limits	4
5.0 Illustrative special cases.....	6
6.0 Implications of preliminary limit group size.....	27
7.0 References.....	27

LIST OF TABLES

Table 1	Time of peak 100-meter concentration and source concentration when $Pe = 10$ for $\lambda' = 3.16, 1, 0.316$ and 0.1	11
---------	--	----

LIST OF FIGURES

Figure 1	Concentration profiles at $t'=1$ for various Pe values: (a) no decay, and (b) decay with $\lambda'=1$. 13	
Figure 2	Concentration profiles at $t'=3.16$ for various Pe values: (a) no decay, and (b) decay with $\lambda'=1$. 14	
Figure 3	Concentration profiles at $t'=10$ for various Pe values: (a) no decay, and (b) decay with $\lambda'=1$. 15	
Figure 4	Breakthrough curves (a) and concentration profiles at the times of the peaks (b) for $Pe=10$: no decay (reference curve), and decay rate $\lambda'=3.16$	16
Figure 5	Breakthrough curves (a) and concentration profiles at the times of the peaks (b) for $Pe=10$: no decay (reference curve), and decay rate $\lambda'=1$	17
Figure 6	Breakthrough curves (a) and concentration profiles at the times of the peaks (b) for $Pe=10$: no decay (reference curve), and decay rate $\lambda'= 0.316$	18
Figure 7	Breakthrough curves (a) and concentration profiles at the times of the peaks (b) for $Pe=10$: no decay (reference curve), and decay rate $\lambda'=0.1$	19
Figure 8	Two-dimensional transport simulation.....	20
Figure 9	Constant tracer source and decaying source of decaying species simulation: plumes.....	21
Figure 10	Constant tracer source and decaying source of decaying species simulation: equidistant breakthrough curves at base.....	22
Figure 11	Constant tracer source and decaying source of decaying species simulation: all breakthrough curves.	23
Figure 12	Constant tracer source and constant source of decaying species simulation: plumes.....	24
Figure 13	Constant tracer source and constant source of decaying species simulation: equidistant breakthrough curves at base.....	25
Figure 14	Constant tracer source and constant source of decaying species simulation: all breakthrough curves.	26

LIST OF ABBREVIATIONS

DU	Disposal unit
PA	Performance Assessment
PIF	Plume interaction factor
SOF	Sum-of-fractions
SRNL	Savannah River National Laboratory
WSRC	Washington Savannah River Company

1.0 Introduction

In the 2008 E-Area Performance Assessment (PA), each *final disposal limit* was constructed as the product of a *preliminary disposal limit* and a *plume interaction factor* (WSRC 2008). The following mathematical development demonstrates that performance objectives are generally expected to be satisfied with high confidence under practical PA scenarios using this method. Pros and cons of analyzing single disposal units or multiple disposal units as a group in the preliminary disposal limits analysis are also identified.

2.0 Preliminary disposal limits

The *performance objective* for a disposal unit (DU) group composed of $J \geq 1$ disposal units is a concentration sum-of-fractions (SOF_C) satisfying the inequality

$$SOF_C(x, t) \equiv \sum_{i=1}^I \sum_{j=1}^J \frac{C_{ij}(x, t)}{C_i^L} \leq 1, \quad (1)$$

where $C_{ij}(x, t)$ is the *actual* 100-meter concentration of species i emanating from disposal unit j , and C_i^L is the concentration (or dose) limit for species i . Herein the term *species* is a shorthand reference to each unique combination of waste form (generic or special) and the most limiting solute within a radionuclide chain. If waste release and solute transport are linear, then superposition can be invoked to rewrite Equation (1) as

$$SOF_C(x, t) = \sum_{i=1}^I \sum_{j=1}^J \frac{m_{ij}c_{ij}(x, t)}{C_i^L} \leq 1, \quad (2)$$

where m_{ij} is the quantity of species i disposed of in DU j , and $c_{ij}(x, t)$ is the 100-meter concentration resulting from a unit mass (mol or Ci) disposal.

For a disposal unit group composed of J disposal units, the *preliminary disposal limit* L_{ij} for species i and disposal unit j (and a specified time window) is defined by

$$\sum_{j=1}^J L_{ij}c_{ij}^L(x, t) \leq \sum_{j=1}^J L_{ij}c_{ij}^L(x_L, t_L) = C_i^L \text{ for } i = 1, \dots, I, \quad (3)$$

where C_i^L is the concentration limit for species i , c_{ij}^L is the 100-meter concentration of species i emanating from disposal unit j in a *Limits* simulation with a unit disposal mass (unit mol or Ci), and (x_L, t_L) is the location/time of the peak concentration. Equation (3) assumes linear transport processes such that superposition holds.

The performance objective, Equation (2), will be satisfied if the disposal facility operates under three constraints. The first constraint is that the disposal inventory sum-of-fractions for each DU j (SOF_{ij}) satisfy the restriction

$$SOF_{Ij} \equiv \sum_{i=1}^I \frac{m_{ij}}{L_{ij}} \leq 1 \text{ for } j = 1, \dots, J. \quad (4)$$

The second constraint is that the waste distribution among disposal units satisfy the proportions

$$\frac{m_{ij}}{\sum_{k=1}^J m_{ik}} = \frac{L_{ij}}{\sum_{k=1}^J L_{ik}} \text{ for } j = 1, \dots, J, \quad (5)$$

or equivalently

$$\frac{m_{ij}}{L_{ij}} = \frac{\sum_{k=1}^J m_{ik}}{\sum_{k=1}^J L_{ik}} \equiv f_i \text{ for } j = 1, \dots, J. \quad (6)$$

Note that the mass fraction m_{ij}/L_{ij} is only a function of species i and not disposal unit j . In other words, the ratio of disposed of mass to disposal limit is constant across disposal units within the group for a given species. Combining Equations (4) and (6) yields

$$SOF_I = \sum_{i=1}^I f_i \leq 1. \quad (7)$$

The third constraint is that

$$c_{ij}(x, t) = c_{ij}^L(x, t), \quad (8)$$

which implies that the *actual* distribution of disposed of waste in space and time within each DU must match the *assumed* spatial/temporal distribution in the limits simulation (to have the same response at 100 meters for all time from a unit mass source).

With these three constraints in place, the performance objective will be satisfied, as demonstrated next. From Equation (8), the concentration SOF_C from Equation (2) can be written

$$SOF_C(x, t) = \sum_{i=1}^I \sum_{j=1}^J \frac{m_{ij} c_{ij}^L(x, t)}{C_i^L}. \quad (9)$$

Multiplying and dividing by the disposal limit yields

$$SOF_C(x, t) = \sum_{i=1}^I \sum_{j=1}^J \frac{\frac{m_{ij}}{L_{ij}} \cdot L_{ij} c_{ij}^L(x, t)}{C_i^L}. \quad (10)$$

Using Equation (6)

$$SOF_C(x, t) = \sum_{i=1}^I \sum_{j=1}^J \frac{f_i \cdot L_{ij} c_{ij}^L(x, t)}{C_i^L}. \quad (11)$$

Because neither f_i and C_i^L are a function of j ,

$$SOF_C(x, t) = \sum_{i=1}^I f_i \frac{\sum_{j=1}^J L_{ij} c_{ij}^L(x, t)}{C_i^L}. \quad (12)$$

Using the Inequality (3),

$$SOF_C(x, t) \leq \sum_{i=1}^I f_i \frac{\sum_{j=1}^J L_{ij} c_{ij}^L(x_L, t_L)}{C_i^L}. \quad (13)$$

Using Equation (3),

$$SOF_C(x, t) \leq \sum_{i=1}^I f_i \frac{C_i^L}{C_i^L} = \sum_{i=1}^I f_i. \quad (14)$$

From Equation (7)

$$SOF_C(x, t) \leq 1, \quad (15)$$

which is the desired outcome.

3.0 Plume interaction factors

The preliminary limits calculation inherently accounts for any co-mingling of plumes emanating from disposal units *within* the analyzed group. *Plume interaction factors (PIF)* can be used to account for further co-mingling or interaction of plumes *among* multiple disposal unit groups.

The plume interaction approach used in the 2008 E-Area Performance Assessment is based on a steady-state tracer (T) simulation, where each disposal unit group J is assigned a constant source term that results in a 100-meter concentration (C_{TJ}) peaking at some limit (C_T^L),

$$C_{TJ}(x) \leq C_{TJ}(x_J) = C_T^L, \quad (16)$$

where x_J is the location of the peak. The tracer source distribution in space, within and among disposal units, is chosen to be the same as in the limits simulation. Dividing by the arbitrary concentration limit yields

$$\frac{C_{TJ}(x)}{C_T^L} \leq \frac{C_{TJ}(x_J)}{C_T^L} = 1, \quad (17)$$

in terms of relative concentrations. Plume interaction factors for multiple disposal unit groups J, K , etc. are defined (non-uniquely) such that

$$\begin{aligned} & PIF_J C_{TJ}(x) + PIF_K C_{TK}(x) + \dots \\ & \leq PIF_J C_{TJ}(x_{JK}) + PIF_K C_{TK}(x_{JK}) + \dots = C_T^L, \end{aligned} \quad (18)$$

where x_{JK} is the location of the peak tracer concentration, distinct from x_j and x_K from Equation (16). Dividing by C_T^L yields

$$\begin{aligned} & PIF_J \frac{C_{TJ}(x)}{C_T^L} + PIF_K \frac{C_{TK}(x)}{C_T^L} + \dots \\ & \leq PIF_J \frac{C_{TJ}(x_{JK})}{C_T^L} + PIF_K \frac{C_{TK}(x_{JK})}{C_T^L} + \dots = 1. \end{aligned} \quad (19)$$

The plume interaction factors may be the same ($PIF_J = PIF_K = \dots$) or different, depending on PA analyst choice.

4.0 Final disposal limits

The performance objective considering all disposal unit groups together is

$$SOF_c(x, t) \equiv \sum_{i=1}^I \sum_{j=1}^J \frac{C_{ij}(x, t)}{C_i^L} + \sum_{i=1}^I \sum_{k=1}^K \frac{C_{ik}(x, t)}{C_i^L} + \dots \leq 1, \quad (20)$$

as applied to each location and time(x, t) along the 100-meter perimeter. This expanded performance objective will generally be satisfied approximately, if not rigorously, if each *final disposal limit* is defined as the product of the preliminary disposal limit and the plume interaction factor for the associated disposal unit group,

$$L_{ij}^f = PIF_J L_{ij}, \quad (21)$$

and the first constraint given by Equation (4) is replaced with

$$SOF_{Ij} \equiv \sum_{i=1}^I \frac{m_{ij}}{L_{ij}^f} \leq 1 \text{ for } j = 1, \dots, J. \quad (22)$$

Using Equation (21), Equation (22) can be recast as

$$\sum_{i=1}^I \frac{m_{ij}}{L_{ij}} \cdot \frac{L_{ij}}{L_{ij}^f} = \sum_{i=1}^I \frac{m_{ij}}{L_{ij}} \cdot \frac{1}{PIF_J} \leq 1, \quad (23)$$

or

$$\sum_{i=1}^I \frac{m_{ij}}{L_{ij}} = \sum_{i=1}^I f_i \leq PIF_J. \quad (24)$$

Satisfaction of the performance objective is considered next. Replacing concentration with source mass times unit mass concentration in Equation (20) yields

$$SOF_C(x, t) = \sum_{i=1}^I \sum_{j=1}^J \frac{m_{ij} c_{ij}^L(x, t)}{C_i^L} + \dots \quad (25)$$

Multiplying and dividing by the preliminary disposal limit produces

$$SOF_C(x, t) = \sum_{i=1}^I \frac{\sum_{j=1}^J \frac{m_{ij}}{L_{ij}} \cdot L_{ij} c_{ij}^L(x, t)}{C_i^L} + \dots \quad (26)$$

From Equation (6)

$$SOF_C(x, t) = \sum_{i=1}^I f_i \frac{\sum_{j=1}^J L_{ij} c_{ij}^L(x, t)}{C_i^L} + \dots \quad (27)$$

The sum in the numerator is the total concentration of species i resulting from J disposal units with the group, C_i^L . Introducing the latter, Equation (27) can be written more concisely as

$$SOF_C(x, t) = \sum_{i=1}^I f_i \frac{C_{ij}^L(x, t)}{C_i^L} + \dots \quad (28)$$

$C_{ij}^L(x, t)/C_i^L$ is the non-dimensional, relative, concentration of species i along the 100-meter perimeter varying between 0 and 1.

Because the preliminary limits and plume interaction simulations use the same (uniform) source term distribution for all species, and all species are subject to the same flow field, the relationship

$$\frac{C_{ij}^L(x, t)}{C_i^L} \leq \frac{C_{TJ}(x)}{C_T^L} \quad (29)$$

is expected to be an accurate approximation, if not rigorous, depending on the species. Intuitively, retardation (resulting from a non-zero sorption coefficient K_d) will affect the timing of solute transport and absolute concentrations for a given mass, but not relative spatial distribution. Radioactive decay and ingrowth will affect absolute concentration and longitudinal distribution, but not lateral distribution; for a 100-meter perimeter that is approximately transverse to the flow direction, the effect of decay and ingrowth will be small. For transient plumes (the most common situation), the peak concentration of each species i will generally occur at different times due to variations in retardation, such that the equality

$$C_{ij}^L(x, t)/C_i^L = C_{TJ}(x)/C_T^L \quad (30)$$

will rarely, if ever, occur simultaneously for all species. The more general condition, due to time separation of peaks, will be

$$C_{ij}^L(x, t)/C_i^L \ll C_{Tj}(x)/C_T^L. \quad (31)$$

Also, Equation (29) pertains to plume interaction factors. If the disposal unit in question is isolated from other units, or interaction with neighboring units is addressed in the preliminary limits analysis, then a plume interaction factor (less than one) is not needed and Equation (29) has no impact.

Beyond these largely intuitive arguments, rigorous proof of the concept embodied by Equation (29) can be established for the special case considered in the next section. Equation (29) is provisionally accepted pending that further investigation. Continuing with the multi-group performance objective $SOFC$, combining Equations (28) and (29) yields

$$SOFC(x, t) \leq \sum_{i=1}^I f_i \frac{C_{Tj}(x)}{C_T^L} + \dots \quad (32)$$

The concentration ratio is not a function of species i , thus

$$SOFC(x, t) \leq \left(\sum_{i=1}^I f_i \right) \left(\frac{C_{Tj}(x)}{C_T^L} \right) + \dots \quad (33)$$

Using Equation (24)

$$SOFC(x, t) \leq PIF_j \frac{C_{Tj}(x)}{C_T^L} + PIF_k \frac{C_{Tk}(x)}{C_T^L} + \dots \quad (34)$$

Combining Equations (19) and (34) yields the desired result,

$$SOFC(x, t) \leq 1. \quad (35)$$

Although similar in appearance, Equation (35) involves multiple disposal unit groups operating under final disposal limits, whereas Equation (15) applies to an isolated disposal unit group operating under preliminary disposal limits. Also, Equation (15) is the result of a rigorous derivation, whereas Equation (35) is based on a key assumption, Equation (29). Although more compelling support for Equation (29) is presented in the next section, this relationship has not been rigorously verified for every transport scenario and can be shown to be invalid under certain conditions identified in the next section. On the other hand, the derivation leading to Equation (35) does not credit time separation of peaks, which constitutes a significant conservatism. On the balance, Equation (35) is expected to be satisfied with high confidence in practice.

5.0 Illustrative special cases

In pursuit of further support for and against Equation (29), consider the single-species solute transport equation set

$$\begin{aligned} R \frac{\partial C_\lambda}{\partial t} &= D \frac{\partial^2 C_\lambda}{\partial x^2} - v \frac{\partial C_\lambda}{\partial x} - R\lambda C_\lambda \\ C_\lambda(0, t) &= \exp(-\lambda t) C_{\lambda 0} \\ C_\lambda(\infty, t) &= 0 \\ C_\lambda(x, 0) &= 0, \end{aligned} \quad (36)$$

where R is retardation factor, D is dispersion/diffusion coefficient, v is pore velocity, and λ is first-order decay constant. The λ subscript on concentration C calls attention to first-order decay of the species (if $\lambda > 0$). For a non-decaying species ($\lambda = 0$), the last term in the partial differential equation drops out, the source term is constant, and a steady-state solution exists, $C_\lambda = C(x)$. For a decaying species, the source term decays and the long-time solution takes the form $C_\lambda = \exp(-\lambda t)C(x)$, as will be demonstrated.

Letting L be the distance to the 100-meter perimeter, then non-dimensional parameters are defined as

$$x' \equiv \frac{x}{L} \quad (37)$$

$$t_a \equiv \frac{LR}{v} \quad (38)$$

$$t' \equiv \frac{t}{t_a} = \frac{t}{LR/v} \quad (39)$$

$$\lambda' \equiv t_a \lambda = \frac{LR}{v} \lambda \quad (40)$$

$$Pe = \frac{vL}{D} \quad (41)$$

$$D' = \frac{D}{vL} = \frac{1}{Pe'} \quad (42)$$

where t_a is advective travel time to the assessment point and Pe is the Peclet number. The equivalent of Equation (40) in terms of half-life is

$$\tau' \equiv \frac{\tau}{t_a} \quad (43)$$

Using the chain rule of differentiation, Equation set (36) becomes

$$R \frac{\partial C_\lambda}{\partial t'} \frac{\partial t'}{\partial t} = D \frac{\partial}{\partial x'} \left[\frac{\partial C_\lambda}{\partial x'} \frac{\partial x'}{\partial x} \right] \frac{\partial x'}{\partial x} - v \frac{\partial C_\lambda}{\partial x'} \frac{\partial x'}{\partial x} - R \lambda C_\lambda$$

$$C_\lambda(0, t) = \exp(-\lambda t) C_{\lambda 0} \quad (44)$$

$$C_\lambda(\infty, t) = 0$$

$$C_\lambda(x, 0) = 0.$$

Replacing dimensional parameters with their non-dimensional counterparts yields

$$R \frac{\partial C_\lambda}{\partial t'} \frac{v}{LR} = vLD' \frac{\partial}{\partial x'} \left[\frac{\partial C_\lambda}{\partial x'} \frac{1}{L} \right] \frac{1}{L} - v \frac{\partial C_\lambda}{\partial x'} \frac{1}{L} - \frac{v}{L} \lambda' C_\lambda$$

$$C_\lambda(0, t') = \exp\left(-\frac{v}{LR} \lambda' \frac{LR}{v} t'\right) C_{\lambda 0} \quad (45)$$

$$C_\lambda(\infty, t') = 0$$

$$C_\lambda(x', 0) = 0,$$

and simplification leaves

$$\frac{\partial C_\lambda}{\partial t'} = D' \frac{\partial^2 C_\lambda}{\partial x'^2} - \frac{\partial C_\lambda}{\partial x'} - \lambda' C_\lambda \quad (46)$$

$$C_\lambda(0, t') = \exp(-\lambda' t') C_{\lambda 0}$$

$$\begin{aligned} C_\lambda(\infty, t') &= 0 \\ C_\lambda(x', 0) &= 0. \end{aligned}$$

Introducing the transform

$$C_\lambda = \exp(-\lambda't') \cdot C \quad (47)$$

yields

$$\begin{aligned} \frac{\partial}{\partial t'} [\exp(-\lambda't)C] &= D' \frac{\partial^2}{\partial x'^2} [\exp(-\lambda't)C] - \frac{\partial}{\partial x'} [\exp(-\lambda't)C] - \lambda' \exp(-\lambda't)C \\ \exp(-\lambda't')C(0, t') &= \exp(-\lambda't')C_{\lambda 0} \\ \exp(-\lambda't')C(\infty, t') &= 0 \\ C(x', 0) &= 0. \end{aligned} \quad (48)$$

Differentiation and simplification produces

$$\begin{aligned} \exp(-\lambda't) \frac{\partial C}{\partial t'} - \exp(-\lambda't) \lambda' C \\ = \exp(-\lambda't) D' \frac{\partial^2 C}{\partial x'^2} - \exp(-\lambda't) \frac{\partial C}{\partial x'} - \exp(-\lambda't) \lambda' C \\ C(0, t') = C_{\lambda 0} \\ C(\infty, t') = 0 \\ C(x', 0) = 0, \end{aligned} \quad (49)$$

which further simplifies to

$$\begin{aligned} \frac{\partial C}{\partial t'} &= D' \frac{\partial^2 C}{\partial x'^2} - \frac{\partial C}{\partial x'} \\ C(0, t') &= C_{\lambda 0} \\ C(\infty, t') &= 0 \\ C(x', 0) &= 0. \end{aligned} \quad (50)$$

Let $C_{\lambda 0} = C_0$ be the source concentration that produces the concentration limit $C = C^L$ at the 100-meter perimeter (not $C_\lambda = C^L$ if the species decays), such that Equation (50) becomes

$$\begin{aligned} \frac{\partial C}{\partial t'} &= D' \frac{\partial^2 C}{\partial x'^2} - \frac{\partial C}{\partial x'} \\ C(0, t') &= C_0 \\ C(\infty, t') &= 0 \\ C(x', 0) &= 0. \end{aligned} \quad (51)$$

Non-dimensional (relative) concentration can be defined as

$$c \equiv \frac{C}{C^L}. \quad (52)$$

Inserting Equation (52) into (51) yields

$$\begin{aligned}
\frac{\partial c}{\partial t'} &= D' \frac{\partial^2 c}{\partial x'^2} - \frac{\partial c}{\partial x'} \\
c(0, t') &= C_0 / C^L \equiv c_0 \geq 1 \\
c(\infty, t') &= 0 \\
c(x', 0) &= 0,
\end{aligned} \tag{53}$$

with c having a peak value of 1.0 at the 100-meter boundary. Therefore, the respective concentrations of a non-decaying species and a tracer species are

$$C_i(x, t') = C_i^L c(x, t') \tag{54}$$

$$C_T(x, t') = C_T^L c(x, t'), \tag{55}$$

where x' has been replaced with x because non-dimensional space is scaled the same for all species. Their relative concentrations thus satisfy

$$\frac{C_i(x, t')}{C_i^L} = \frac{C_T(x, t')}{C_T^L}. \tag{56}$$

Thus, Equation set (53) demonstrates that the relative concentration of a non-decaying species is identical to that of any other non-decaying species, including a non-sorbing tracer, in non-dimensional time and dimensional space. Concentration peaks when steady-state conditions are reached ($t \rightarrow \infty$), so that

$$\frac{C_i(x, t)}{C_i^L} \leq \frac{C_i(x, \infty)}{C_i^L} = \frac{C_T(x, \infty)}{C_T^L}, \tag{57}$$

in agreement with Equation (29). Therefore, Equation (29) is rigorously correct for a non-decaying species for the considered scenario. For a decaying species, this is not the case as shown next.

For a decaying species, a larger initial source concentration is required to produce $C_\lambda = C^L$ (rather than $C = C^L$) at the 100-meter perimeter, due to decay between the source and perimeter. Let $C_{\lambda 0} = C_1$ be the source concentration that produces the concentration limit $C_\lambda = C^L$ at the 100-meter perimeter, such that Equation (50) becomes

$$\begin{aligned}
\frac{\partial C^*}{\partial t'} &= D' \frac{\partial^2 C^*}{\partial x'^2} - \frac{\partial C^*}{\partial x'} \\
C^*(0, t') &= C_1 \\
C^*(\infty, t') &= 0 \\
C^*(x', 0) &= 0,
\end{aligned} \tag{58}$$

where C is replaced with C^* to avoid confusion with Equation set (51), which has a different source term. Define non-dimensional (relative) concentration for the decaying species as

$$c_\lambda \equiv \frac{C_\lambda}{C^L} \tag{59}$$

and for its non-decaying counterpart

$$c^* \equiv \frac{C^*}{C^L}. \quad (60)$$

Then

$$\begin{aligned} \frac{\partial c^*}{\partial t'} &= D' \frac{\partial^2 c^*}{\partial x'^2} - \frac{\partial c^*}{\partial x'} \\ c^*(0, t') &= C_1/C^L \equiv c_1 > c_0 \geq 1 \\ c^*(\infty, t') &= 0 \\ c^*(x', 0) &= 0. \end{aligned} \quad (61)$$

Note that

$$\frac{C^*}{C} = \frac{C_1}{C_0} = \frac{c^*}{c} = \frac{c_1}{c_0} \geq 1. \quad (62)$$

Dividing Equation (47) by C^L and using Equation (59) yields

$$c_\lambda = \exp(-\lambda' t') \cdot \frac{C^*}{C^L} = \exp(-\lambda' t') \frac{C^*}{C} \frac{C}{C^L}. \quad (63)$$

Introducing Equations (52) and (62) yields

$$c_\lambda = \exp(-\lambda' t') \frac{C_1}{C_0} c. \quad (64)$$

Then for each general decaying species i

$$C_{\lambda i}(x, t') = C_i^L c_\lambda(x, t') = C_i^L \exp(-\lambda' t') \frac{C_1}{C_0} c(x, t'), \quad (65)$$

or in terms of concentration relative to its peak value,

$$\frac{C_{\lambda i}(x, t')}{C_i^L} = \exp(-\lambda' t') \frac{C_1}{C_0} \cdot \frac{C_T(x, t')}{C_T^L}. \quad (66)$$

The relationship between $C_{\lambda i}(x, t')/C_i^L$ and $C_T(x, \infty)/C_T^L$, akin to Equation (57), is not clear from Equation (66).

Insight may be gained by examining the one-dimensional analytic solution to Equation set (50), which was derived by Ogata and Banks (1961) as

$$C = C_{\lambda 0} \left[\operatorname{erfc} \left(\frac{1-t'}{\sqrt{4D't'}} \right) + \exp \left(\frac{x'}{D'} \right) \operatorname{erfc} \left(\frac{1+t'}{\sqrt{4D't'}} \right) \right], \quad (67)$$

as summarized by Bear (1972, Equation (10.6.22)) in dimensional form. Then from Equation (47)

$$C_\lambda = C_{\lambda 0} \exp[-\lambda' t'] \left[\operatorname{erfc} \left(\frac{1-t'}{\sqrt{4D't'}} \right) + \exp \left(\frac{x'}{D'} \right) \operatorname{erfc} \left(\frac{1+t'}{\sqrt{4D't'}} \right) \right]. \quad (68)$$

Figure 1 through Figure 3 illustrate Equation (68) for $\lambda' = 0$ and 1 and various other parameter settings. Note the different scales of the vertical axes for the no-decay ($\lambda' = 0$) and $\lambda' = 1$ cases.

Figure 4 through Figure 7 illustrate breakthrough curves and concentration profiles for the no-decay ($\lambda' = 0$) and decay ($\lambda' > 0$) cases defined by Equation sets (53) and (61), respectively, for $\lambda' = 3.16, 1, 0.316$ and 0.1 ($10^{0.5}, 10^0, 10^{-0.5}$ and 10^{-1}). Advection-dominated transport typical of field-scale transport is assumed through the selection $Pe = 10$. For one-dimensional transport, $c_0 = 1$ and $c_1 > 1$. For the decaying species, Table 1 lists the time when the peak concentration occurs at 100-meters and the source concentration required to achieve $c_\lambda = 1$ at that assessment point.

Table 1 Time of peak 100-meter concentration and source concentration when $Pe = 10$ for $\lambda' = 3.16, 1, 0.316$ and 0.1 .

Decay rate, λ'	Time of peak, t'	Source concentration, c_1
$10^{0.5} = 3.16$	0.75	32.7
$10^0 = 1$	1.12	4.49
$10^{-0.5} = 0.316$	1.58	1.84
$10^{-1} = 0.1$	2.00	1.26

For a non-decaying species, the peak 100-meter ($x' = 1$) concentration ($c = 1$) occurs when steady-state conditions ($t' \rightarrow \infty$) are achieved (blue lines in upper plots of Figure 4 through Figure 7). At that time, upgradient ($x' < 1$) and downgradient ($x' > 1$) concentrations are also $c = 1$ (blue lines in lower plots of Figure 4 through Figure 7). For a decaying species, the time of the peak concentration depends on the decay rate, λ' (orange lines in upper plots of Figure 4 through Figure 7). At the times of these peak 100-meter concentrations, upgradient concentrations are greater than 1.0 and downgradient concentrations are less than 1.0 (orange lines in lower plots of Figure 4 through Figure 7):

$$\frac{C_{\lambda i}(x' < 1, t')}{C_i^L} > \frac{C_T(x', \infty)}{C_T^L} \quad (69)$$

$$\frac{C_{\lambda i}(x' > 1, t')}{C_i^L} < \frac{C_T(x', \infty)}{C_T^L}. \quad (70)$$

While Equation (29) is not valid for arbitrary x when the solute decays, Equation (29) is nonetheless expected to hold under practical PA scenarios, for multiple reasons:

1. For most nuclides $\lambda' \ll 1$. Under this condition relative concentrations of the decaying species only slightly exceed those of the non-decaying tracer (orange versus blue lines in Figure 7(b)).
2. The 100-meter perimeter tends to run transverse to the flow direction, such that at the time of the peak (t'_{100m}) all positions along the 100-perimeter (x'_{100m}) are the same distance (travel time) from the source zone and

$$\frac{C_{\lambda i}(x'_{100m}, t'_{100m})}{C_i^L} \cong \frac{C_T(x', \infty)}{C_T^L}. \quad (71)$$

If the 100-meter is not strictly orthogonal to the flow direction, then location of the peak concentration tends to be closest to the source, with other positions further away (downgradient). In this case,

$$\frac{C_{\lambda i}(x'_{100m}, t'_{100m})}{C_i^L} \leq \frac{C_T(x', \infty)}{C_T^L} \quad (72)$$

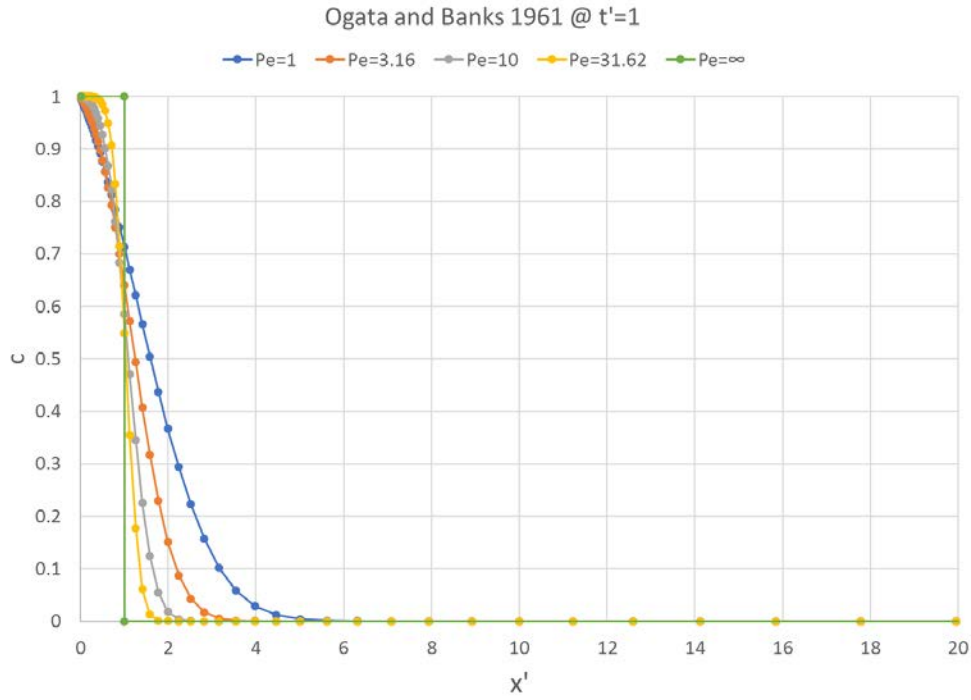
is the expected result per Equation (70).

One challenging nuclide is H-3 with $\tau = 12.3$ years or $\lambda = \ln(2)/\tau = 0.0564$ 1/yr. In E-Area the travel time to the 100-meter assessment point for tritium at least $t_a = 15$ years. The non-dimensional decay rate is then $\lambda' = t_a \lambda \geq 15 \times 0.0564 = 0.85 \approx 1$. For this condition, the upgradient concentration for the decaying species can be significantly greater than 1.0 (Figure 4(b) and Figure 5(b)). If H-3 constitutes most of the disposal inventory in multiple adjoining disposal units, preliminary limits are based on individual units ($J = 1$), and the 100-meter perimeter mimics the shape of H-3 plume concentration contours, then

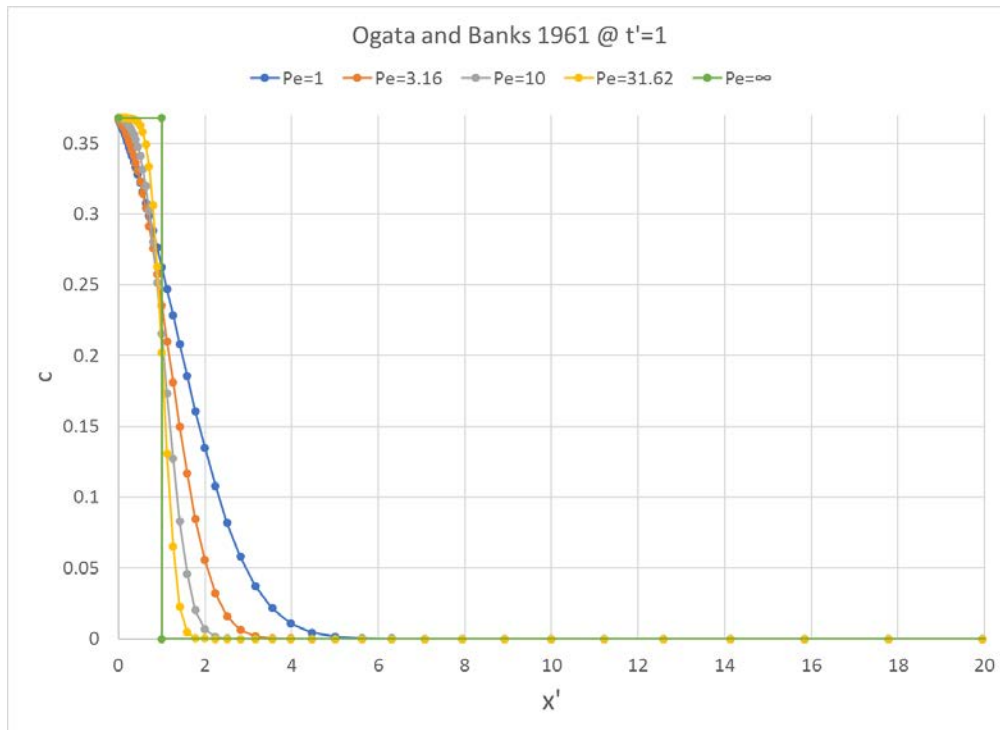
$$\frac{C_{\lambda i}(x'_{100m}, t'_{100m})}{C_i^L} > \frac{C_T(x', \infty)}{C_T^L} \quad (73)$$

may be the case per Equation (69), contrary to Equation (29). However, Equation (35) will likely still hold due to time separation of peaks.

A more challenging nuclide is Sr-90. Although the decay rate of Sr-90 is significantly slower than H-3, its retarded travel time is much larger. Assuming sorption coefficient $K_d = 5$ mL/g, bulk density $\rho_b = 1.6$ g/mL, and porosity $n = 0.4$, the retardation factor is $R = 1 + \rho_b K_d / n = 21$. The retarded travel time becomes $21 \times 15 = 315$ years, and the non-dimensional decay rate is $\lambda' = 7.6 \gg 1$.

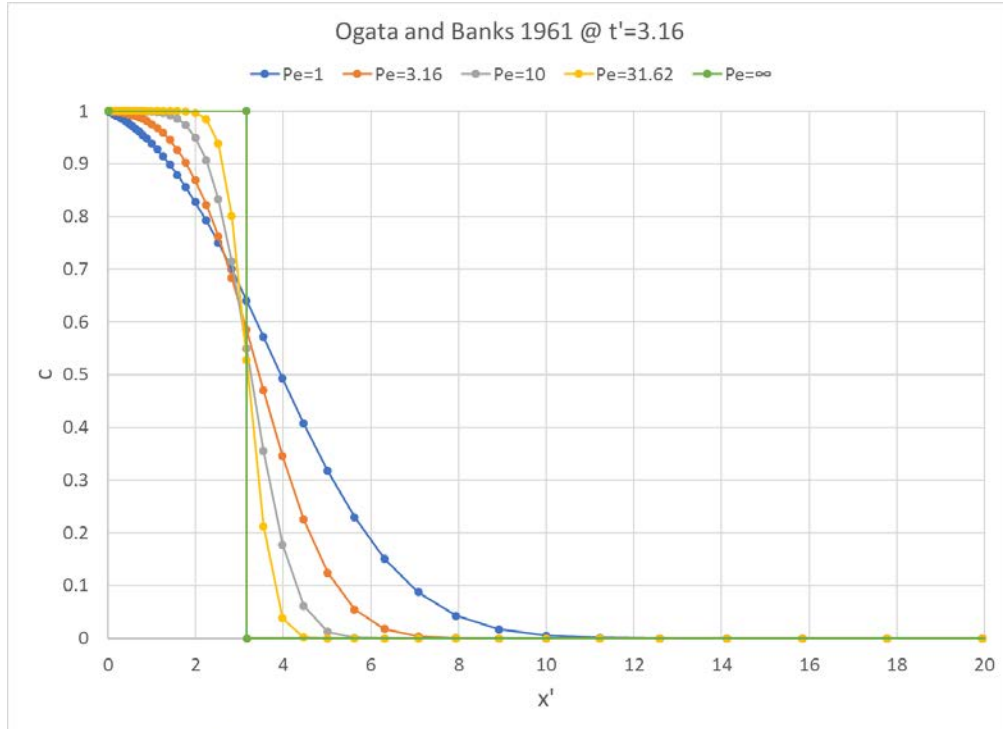


(a)

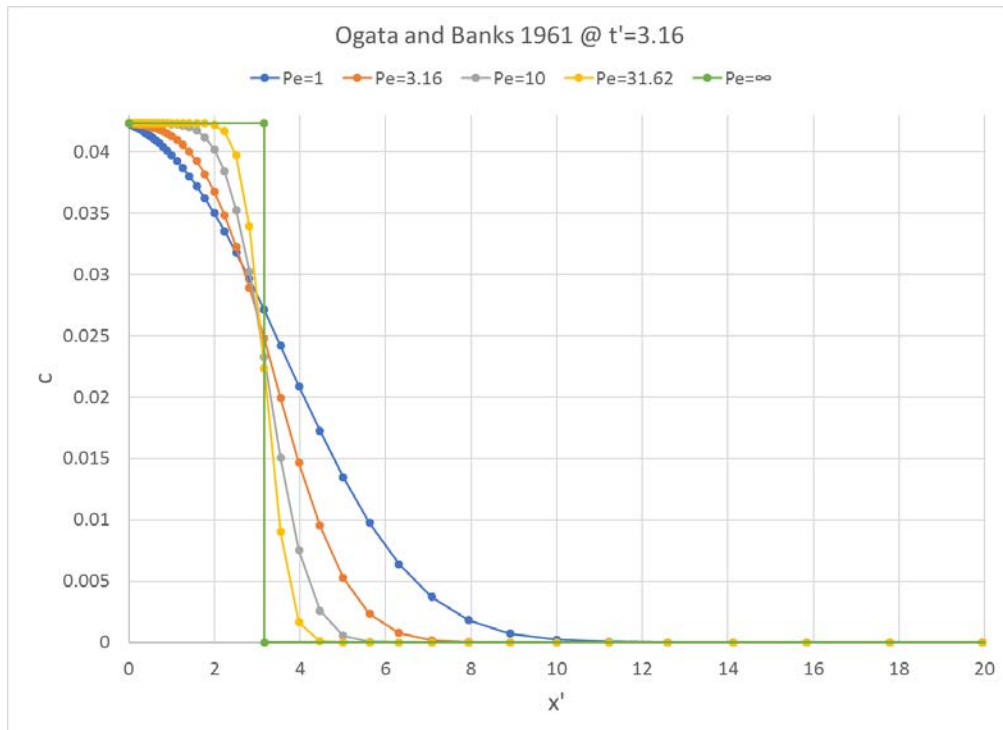


(b)

Figure 1 Concentration profiles at $t'=1$ for various Pe values: (a) no decay, and (b) decay with $\lambda'=1$.

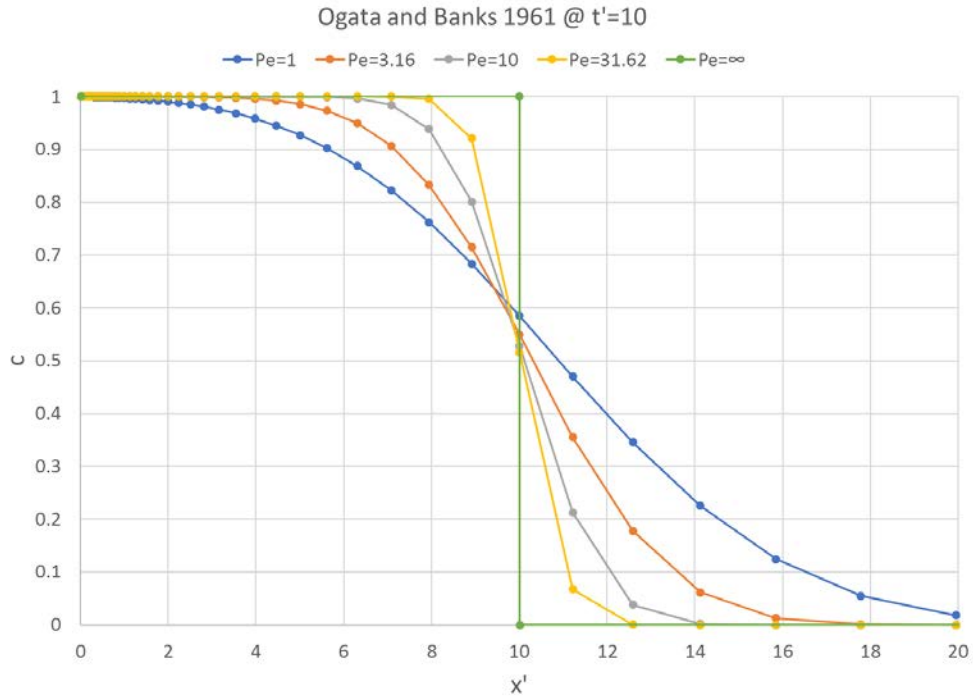


(a)

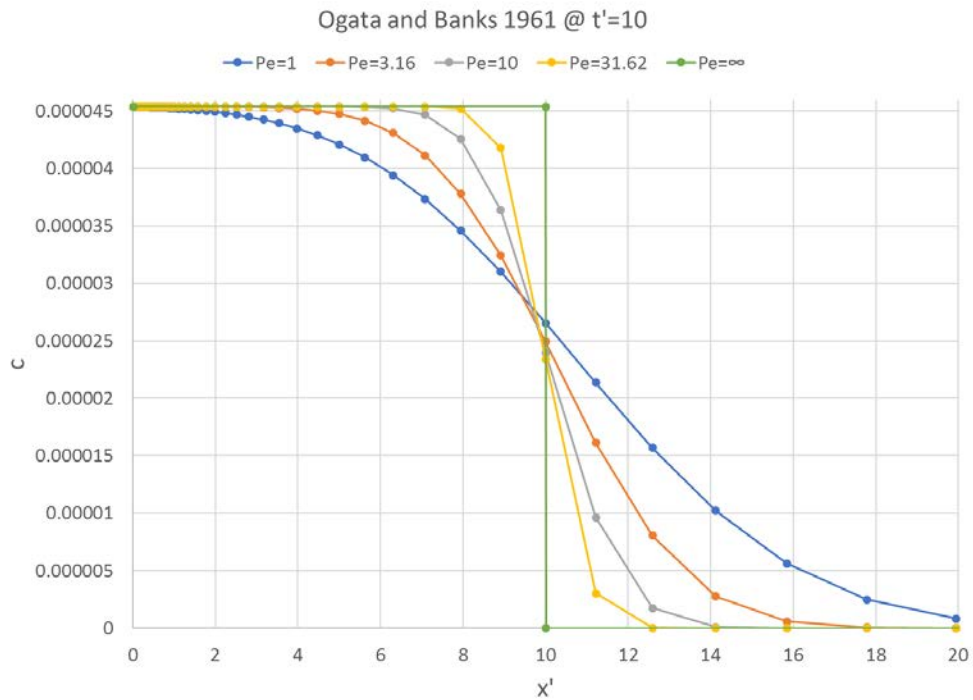


(b)

Figure 2 Concentration profiles at $t'=3.16$ for various Pe values: (a) no decay, and (b) decay with $\lambda'=1$.

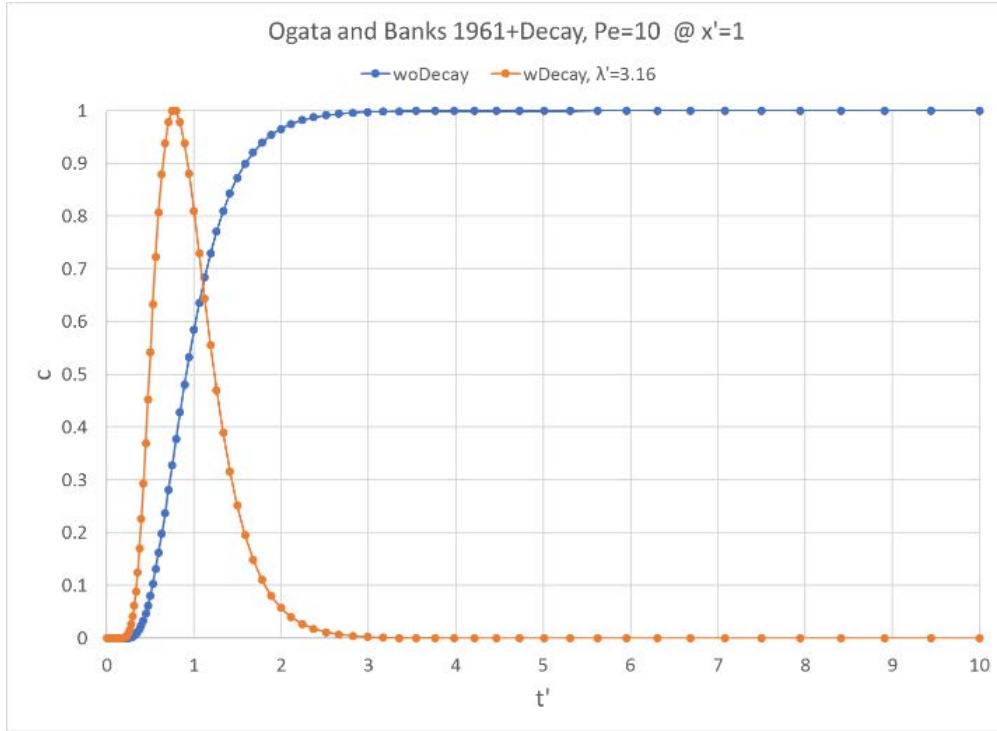


(a)

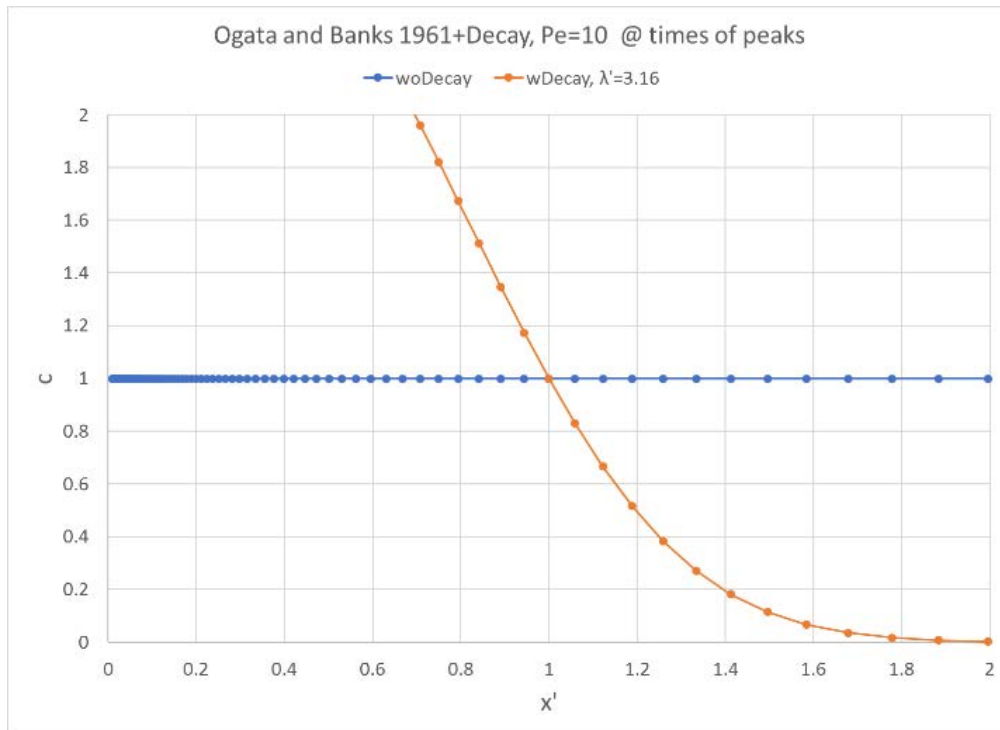


(b)

Figure 3 Concentration profiles at $t'=10$ for various Pe values: (a) no decay, and (b) decay with $\lambda'=1$.

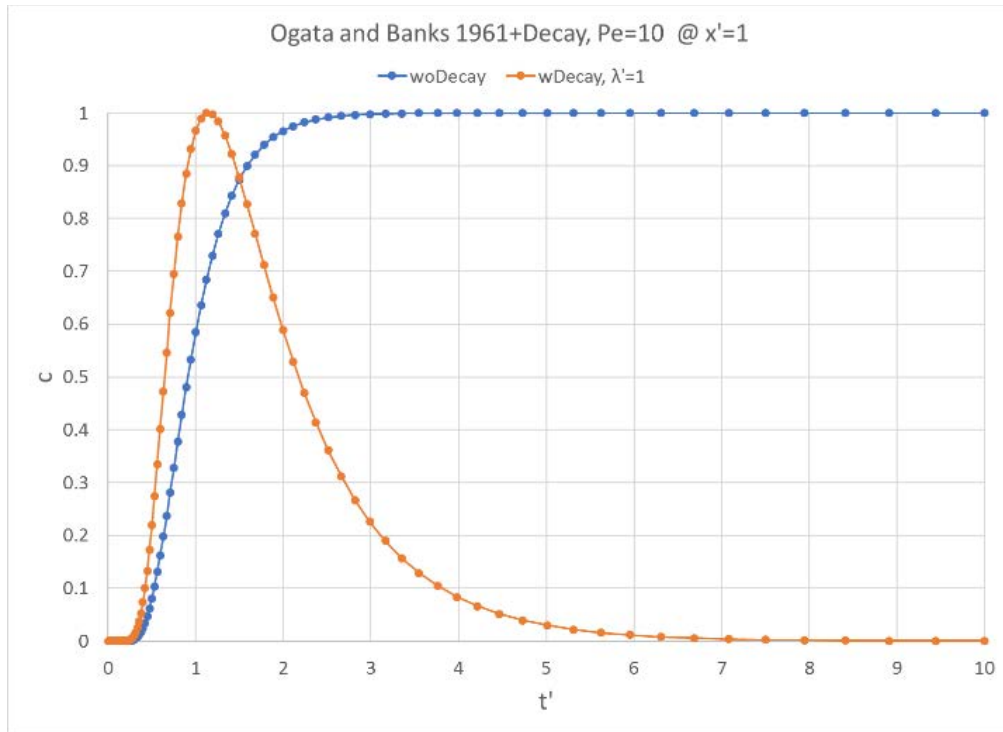


(a)

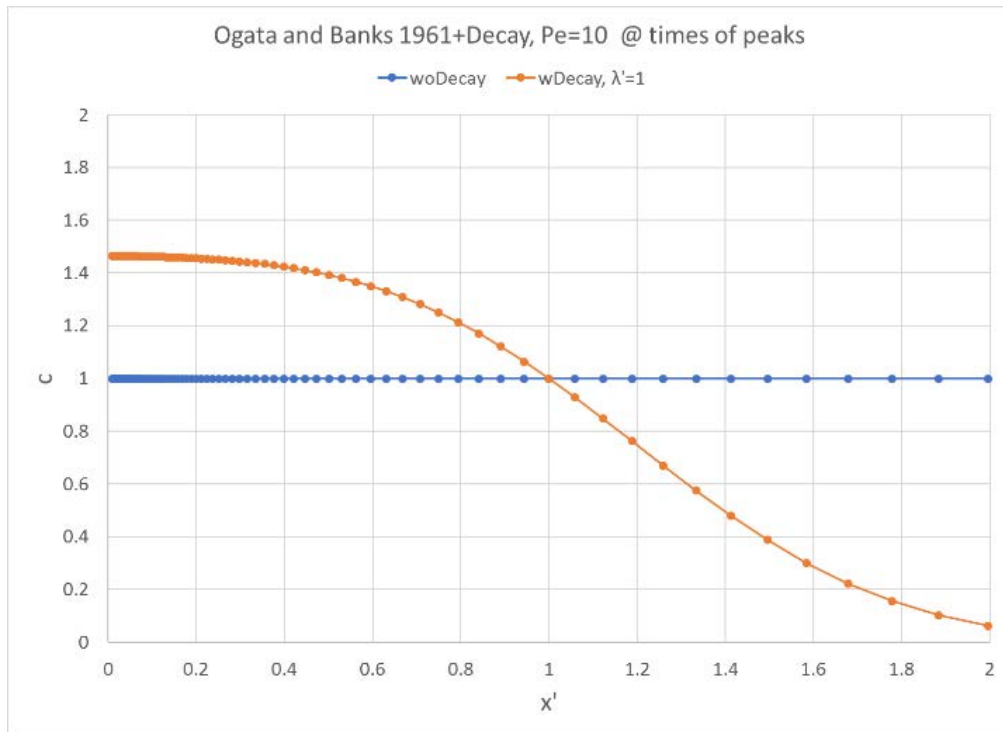


(b)

Figure 4 Breakthrough curves (a) and concentration profiles at the times of the peaks (b) for $Pe=10$: no decay (reference curve), and decay rate $\lambda'=3.16$.

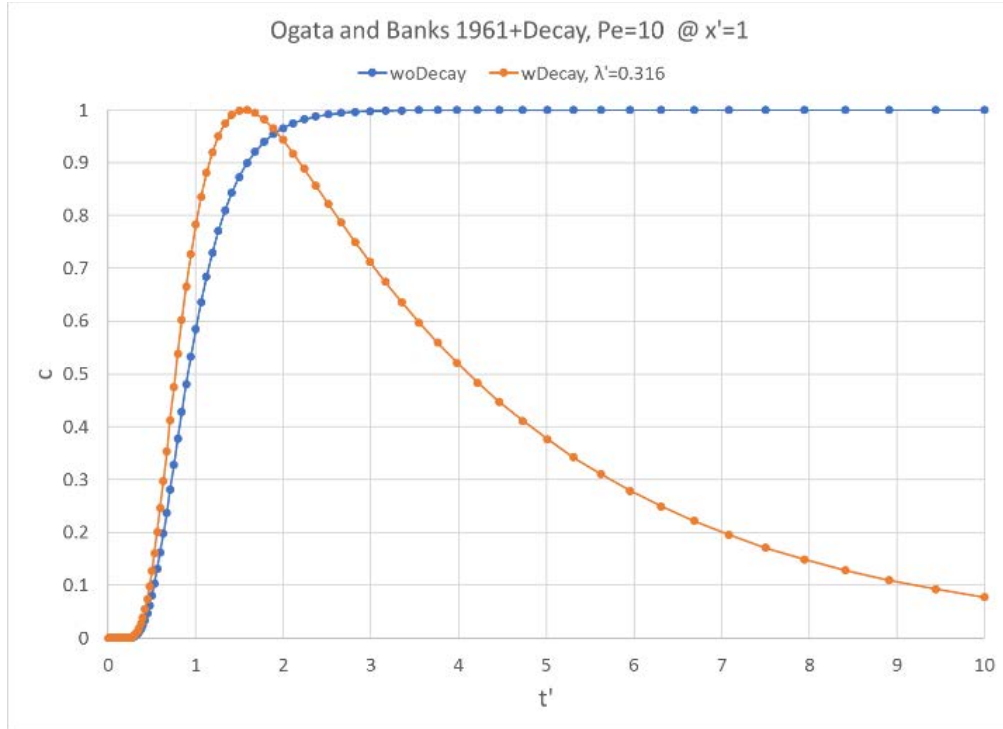


(a)

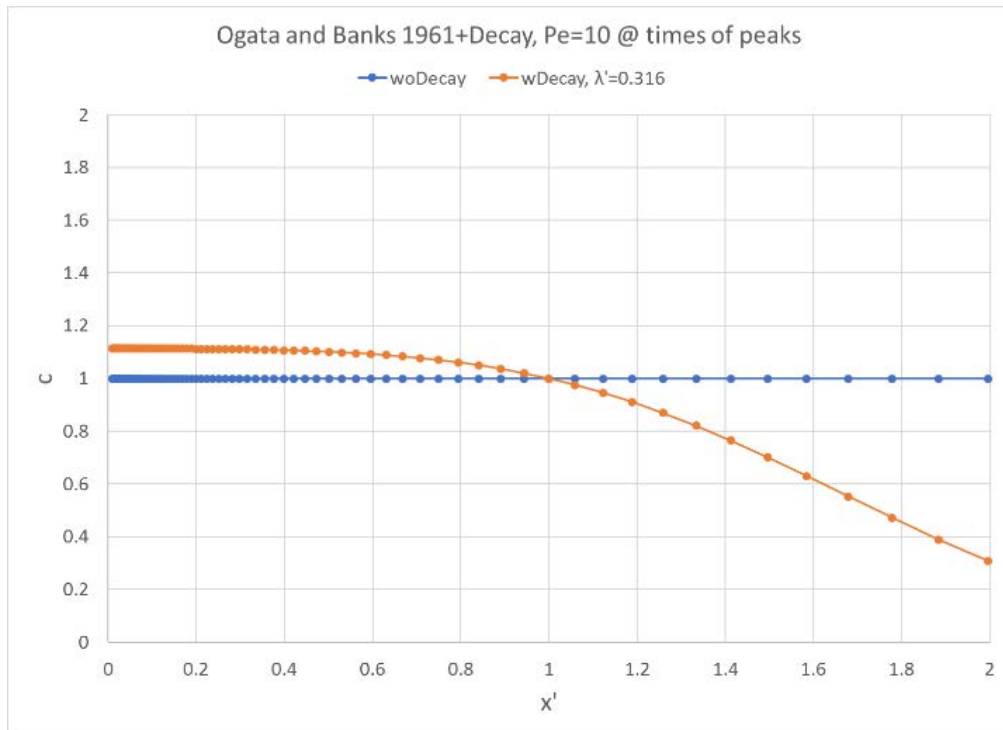


(b)

Figure 5 Breakthrough curves (a) and concentration profiles at the times of the peaks (b) for $Pe=10$: no decay (reference curve), and decay rate $\lambda'=1$.

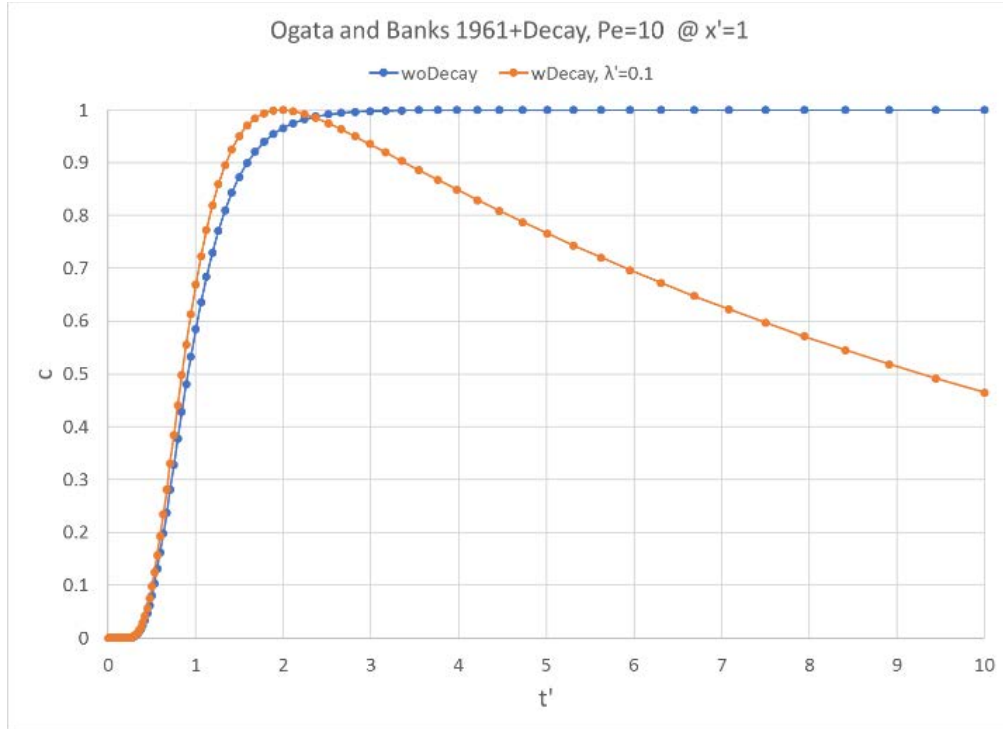


(a)

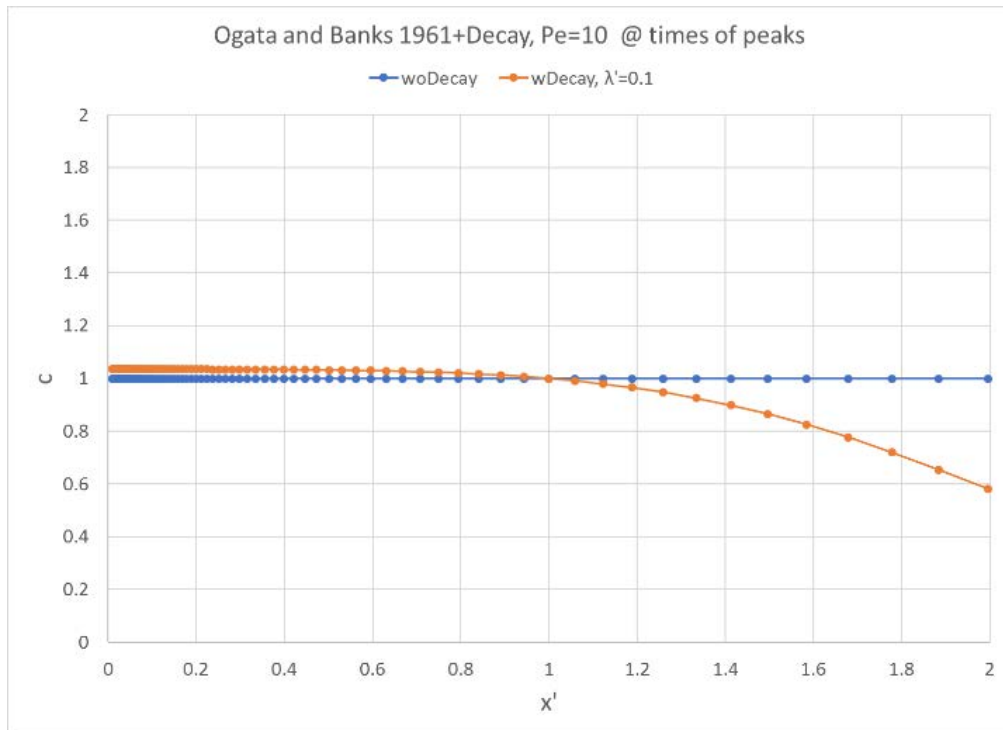


(b)

Figure 6 Breakthrough curves (a) and concentration profiles at the times of the peaks (b) for $Pe=10$: no decay (reference curve), and decay rate $\lambda'=0.316$.



(a)



(b)

Figure 7 Breakthrough curves (a) and concentration profiles at the times of the peaks (b) for $Pe=10$: no decay (reference curve), and decay rate $\lambda'=0.1$.

To illustrate and expand upon the insights gained from the above one-dimensional analytic solution, two-dimensional numerical simulations are presented next. Figure 8 defines the problem setup. Two species are simulated: a nonsorbing and nondecaying tracer, and a nonsorbing but decaying species with half-life $\tau = 10$ years. Travel time to the base of the model domain is 100 years, so $\lambda' = 10 \ln(2) = 6.9$, which is similar to Sr-90 in E-Area ($\lambda' = 7.6$). Longitudinal and transverse dispersivities are set to 10% and 1% of the plume travel length, respectively. Two cases are considered with respect to the decaying species: a decaying mass source starting at 1 Ci/yr analogous to the decaying concentration in Equation (36), and a non-depleting source constant at 1 Ci/yr. A scaling factor of 25 is applied to concentrations so that the peak tracer concentration is 1.0 Ci/m³ in plots.

Figure 9 illustrates the steady-state tracer plume and the decaying species plume at the time when its concentration peaks at 100 meters, 102 years. Also shown in the figure are several observation nodes aligned with the center and edge of the source zone. Figure 10 shows breakthrough curves at 100 meters. The ratio of the edge concentration to the center concentration is practically the same for both species, which is expected for observation nodes equidistant from the source. Figure 11 illustrates the breakthrough curves for all observation nodes. When the tracer plume reaches steady-state, the ratio of all five edge concentrations to the peak 100 meter concentration (C_{50}) is about 0.57. For the decaying species, the ratio of C_{75} to C_{50} is 0.54 (≈ 0.57 , as observed from Figure 10). However, as the distance between the edge node and source zone decreases, the ratio of peak edge concentration to peak 100 meter center concentration increases, as expected based on insights gained from the 1D analytic solution.

Similar behaviors occur when the decaying species source is non-depleting/constant; see Figure 12 through Figure 14. These two-dimensional simulations support generalization of Equations (69) and (70) to multiple dimensions.

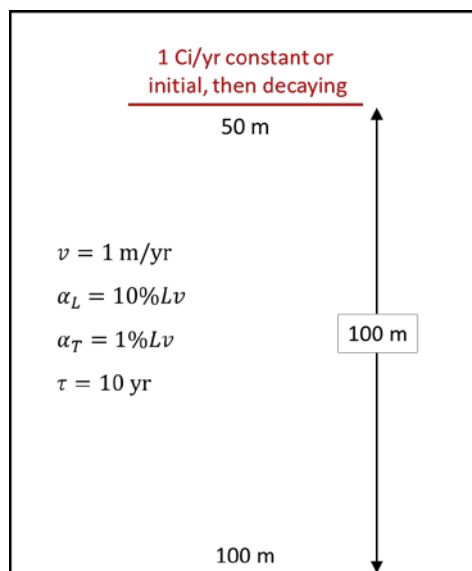


Figure 8 Two-dimensional transport simulation.

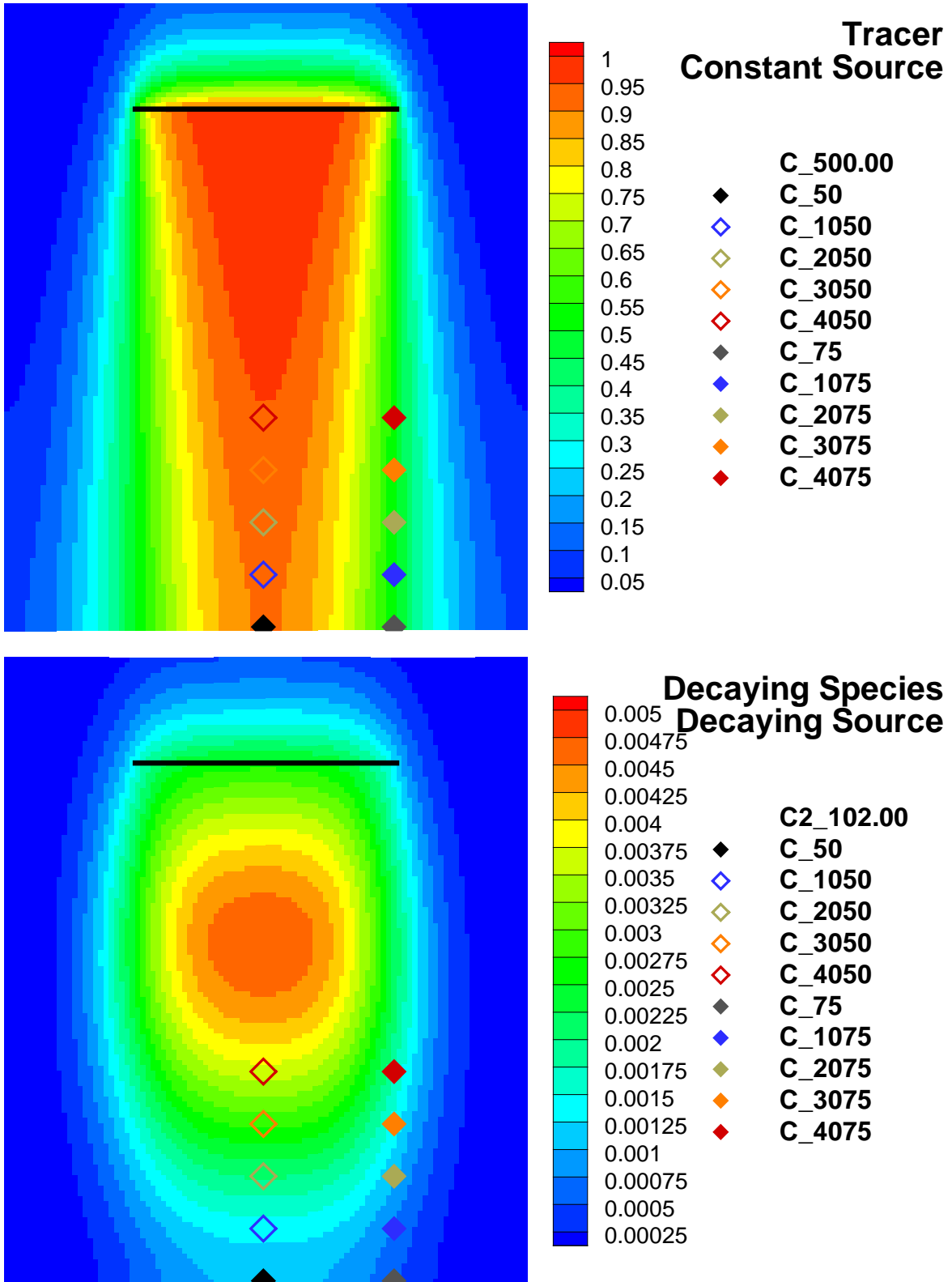


Figure 9 Constant tracer source and decaying source of decaying species simulation: plumes.

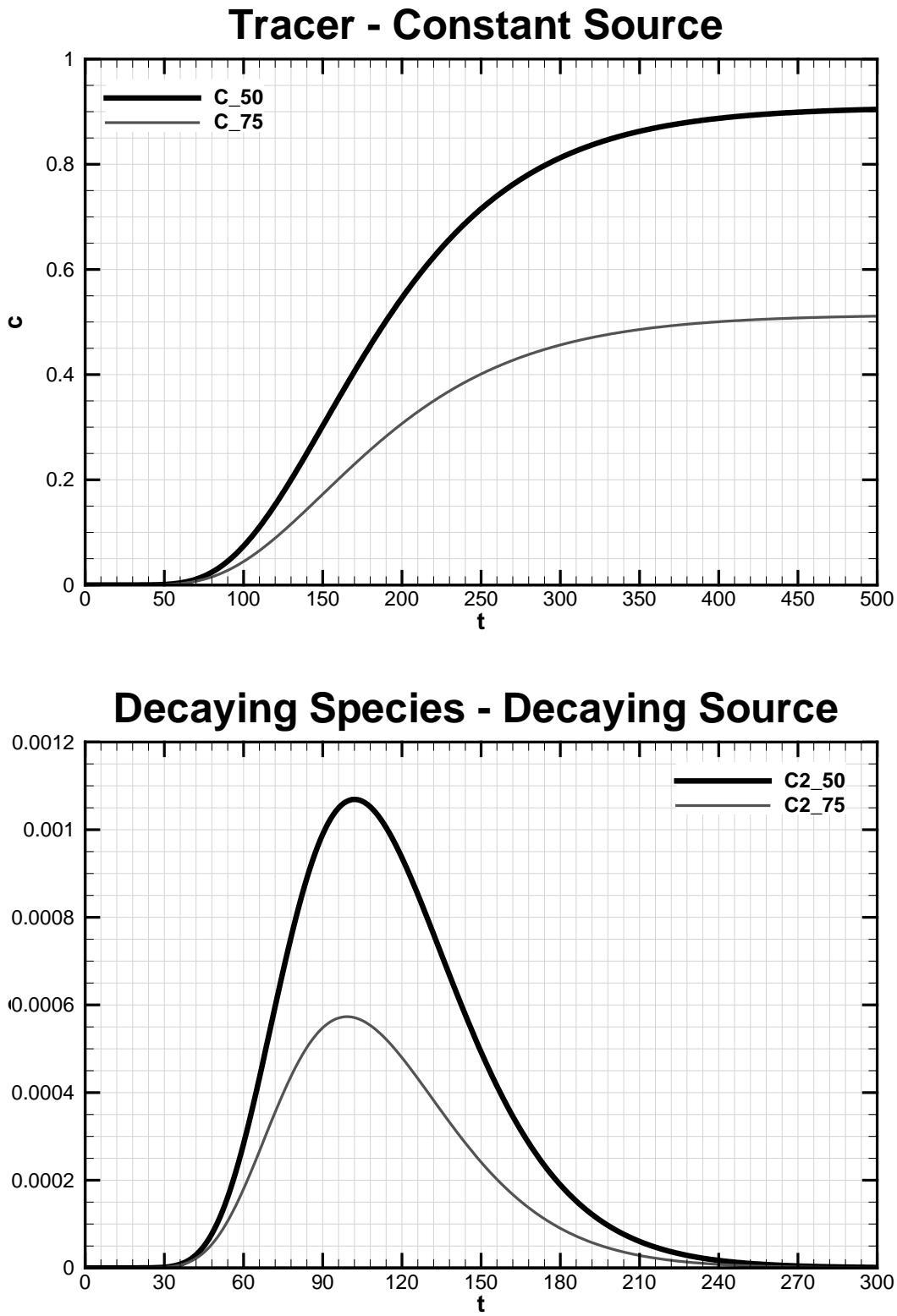


Figure 10 Constant tracer source and decaying source of decaying species simulation: equidistant breakthrough curves at base.

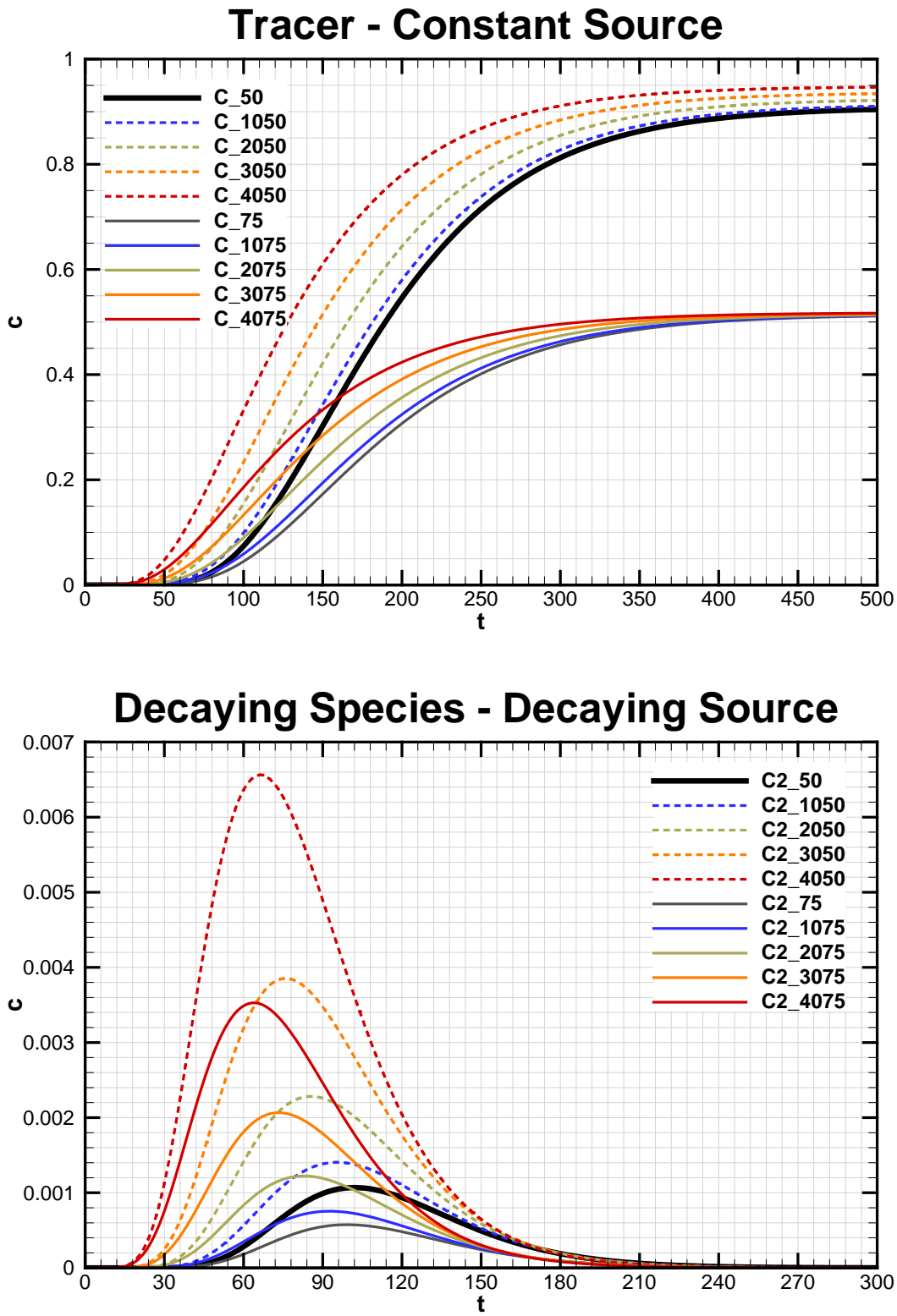


Figure 11 Constant tracer source and decaying source of decaying species simulation: all breakthrough curves.

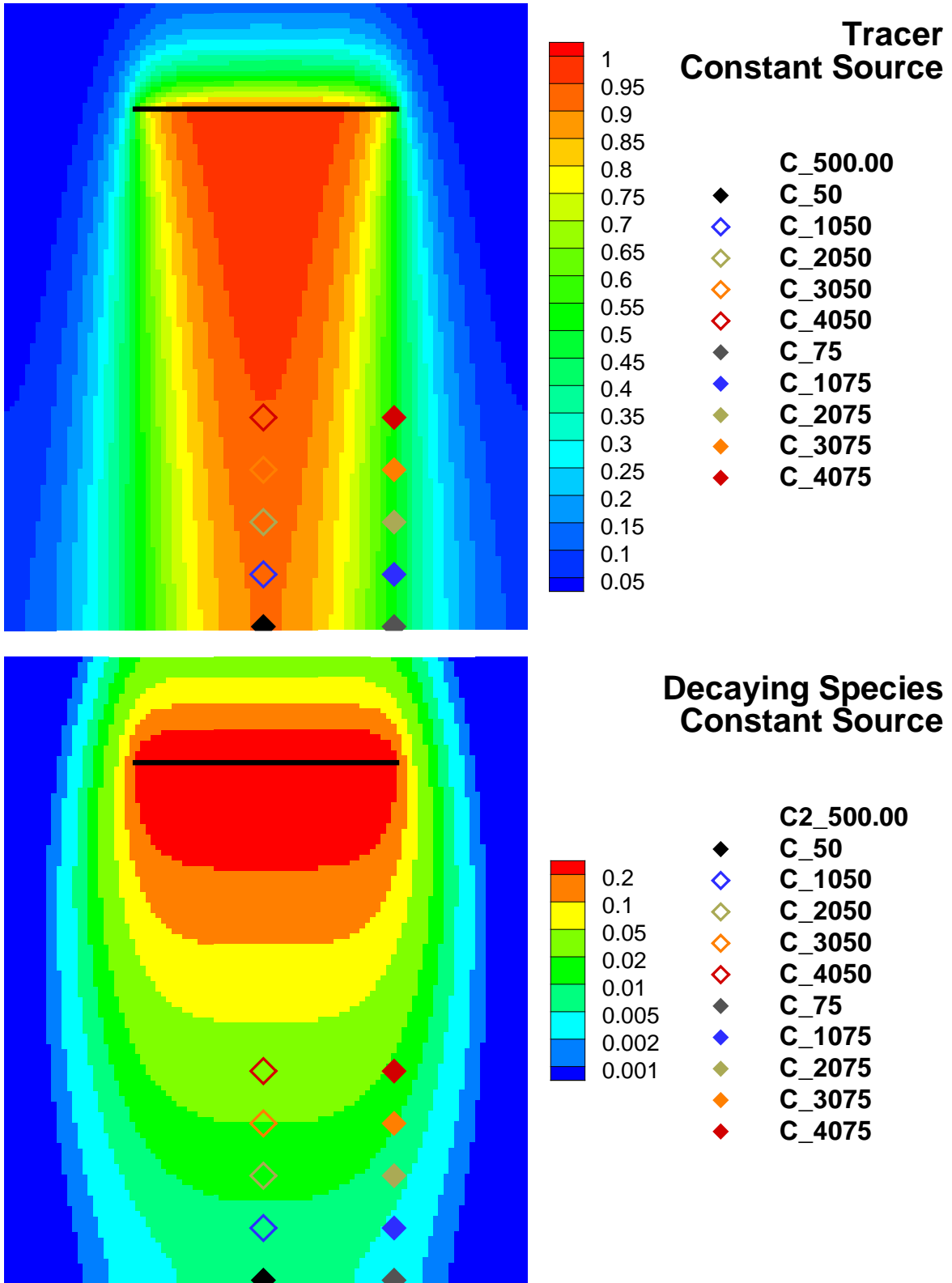


Figure 12 Constant tracer source and constant source of decaying species simulation: plumes.

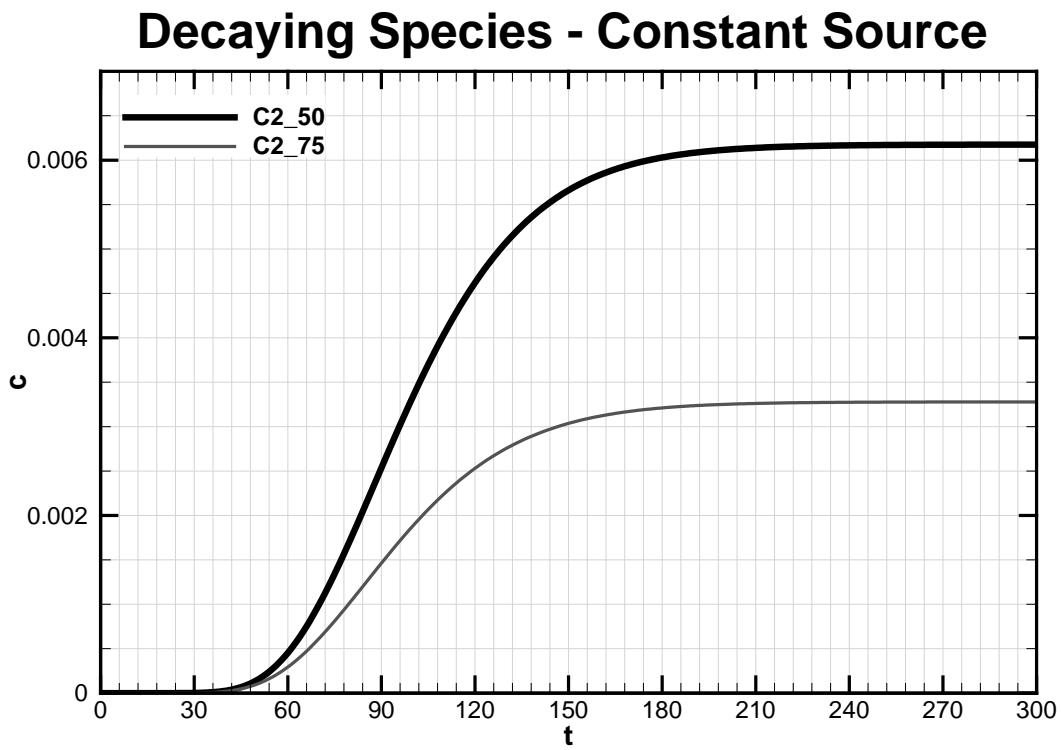
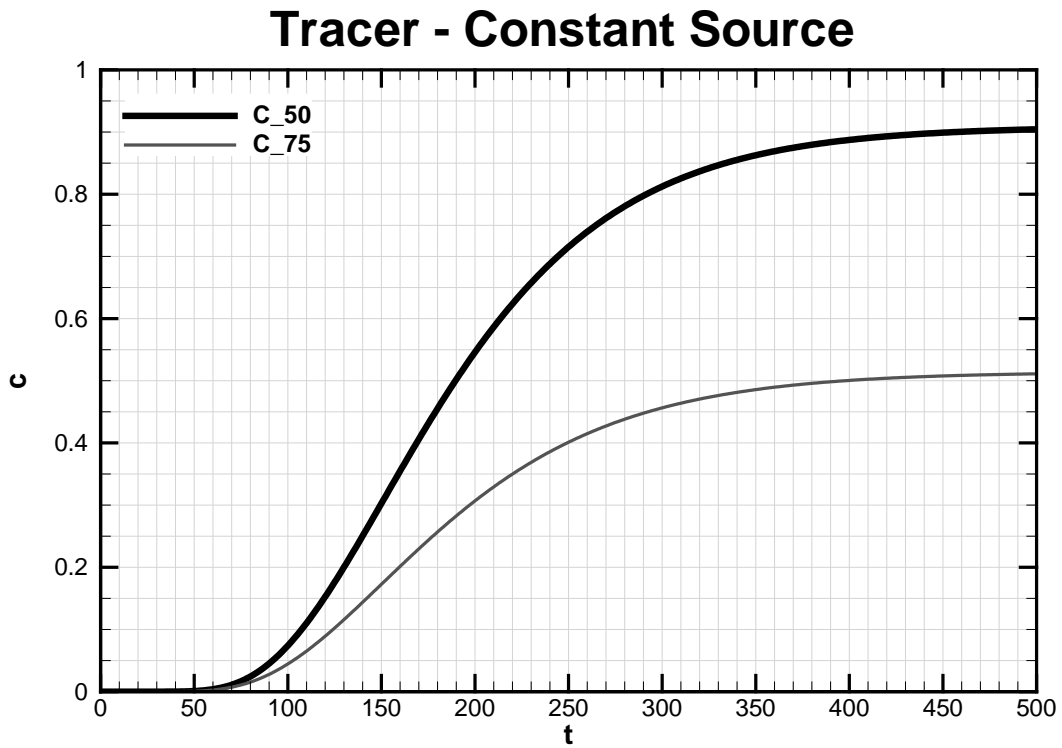


Figure 13 Constant tracer source and constant source of decaying species simulation: equidistant breakthrough curves at base.

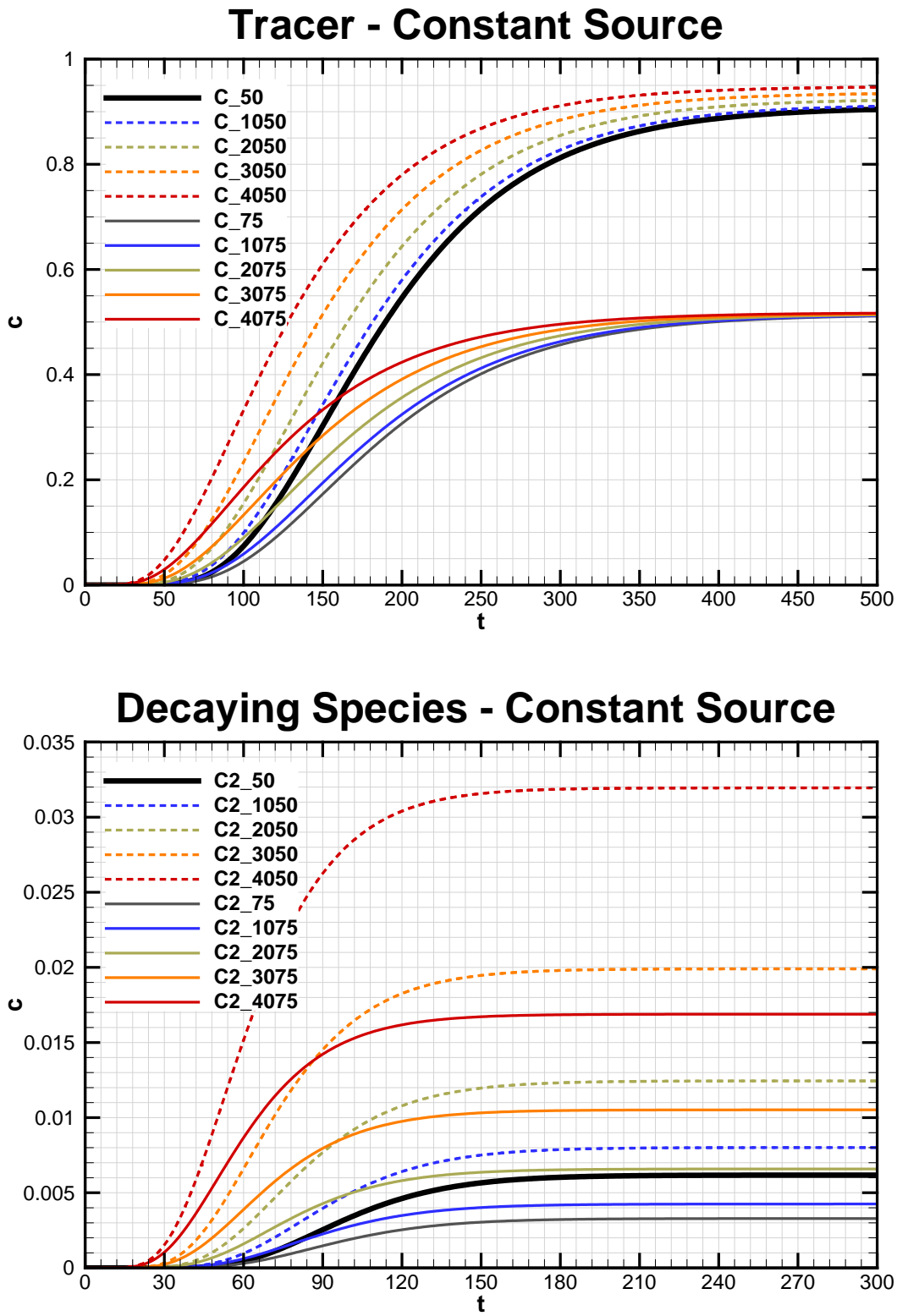


Figure 14 Constant tracer source and constant source of decaying species simulation: all breakthrough curves.

6.0 Implications of preliminary limit group size

The disposal unit group in the preliminary limits calculation can comprise a single unit ($J = 1$), a few units ($J > 1$), or many units ($J \gg 1$). Advantages and disadvantages are associated with each end-member.

When all units with co-mingling plumes are analyzed as a group ($J \gg 1$), then interactions with additional units are non-existent, plume interaction factors are irrelevant, and the assumption given by Equation (29) is never invoked. Time separation of peaks is fully credited with this approach, resulting in the second advantage of higher disposal limits. The disadvantage is that disposal operations become constrained by Equation (6), and Equation (8) applied to each unit in the group.

When a single unit is analyzed in the preliminary limits calculation ($J = 1$), the operational constraint given by Equation (6) does not exist and operations are only constrained by Equation (8) for the immediate disposal unit. That is, operations for the disposal unit are not coupled to operations in neighboring units. However, the plume interaction factor based on the assumption given by Equation (29) becomes a significant component of the final limits, and no credit is taken for time separation of peaks, which results in lower disposal limits.

An intermediate group size results in a blending of these pros and cons.

A group size of one ($J = 1$), that is, preliminary limits based on analysis of a single disposal unit in isolation, is preferred if the lower disposal limits are acceptable. If higher disposal limits are needed, then group size should be increased to the minimum extent required to achieve the desired limits. It is further suggested that all concentration time history be captured at the 100-meter perimeter in the group-size-of-one simulations to facilitate super-positioning of peaks should group size need to be increased.

7.0 References

Bear, J. *Dynamics of Fluids in Porous Media*. Dover Publications. New York. 764 p. 1972.

Ogata, A. and R. B. Banks. *A solution of the differential equation of longitudinal dispersion in porous media*. U. S. Geological Survey Professional Paper 411-A. 1961.

Washington Savannah River Company LLC. *E-Area Low-Level Waste Facility DOE 435.1 Performance Assessment*. WSRC-STI-2007-00306, Rev. 0. July 2008.

Distribution:

timothy.brown@srnl.doe.gov
michael.cercy@srnl.doe.gov
alex.cozzi@srnl.doe.gov
david.crowley@srnl.doe.gov
david.dooley@srnl.doe.gov
a.fellinger@srnl.doe.gov
samuel.fink@srnl.doe.gov
erich.hansen@srnl.doe.gov
connie.berman@srnl.doe.gov
david.berman@srnl.doe.gov
elizabeth.hoffman@srnl.doe.gov
kevin.fox@srnl.doe.gov
john.mayer@srnl.doe.gov
daniel.mccabe@srnl.doe.gov
nancy.halverson@srnl.doe.gov
frank.pennebaker@srnl.doe.gov
william.ramsey@srnl.doe.gov
luke.reid@srnl.doe.gov
geoffrey.smoland@srnl.doe.gov
michael.stone@srnl.doe.gov
boyd.wiedenman@srnl.doe.gov
bill.wilmarth@srnl.doe.gov
Records Administration (EDWS)

tom.butcher@srnl.doe.gov
tim.coffield@srs.gov
thomas.danielson@srnl.doe.gov
james.dyer@srnl.doe.gov
gregory.flach@srnl.doe.gov
lee.fox@srs.gov
luther.hamm@srnl.doe.gov
thong.hang@srnl.doe.gov
ginger.humphries@srs.gov
vijay.jain@srs.gov
daniel.kaplan@srnl.doe.gov
dien.li@srs.gov
larry.romanowski@srs.gov
kent.rosenberger@srs.gov
roger.seitz@srnl.doe.gov
ira.stewart@srs.gov
kevin.tempel@srs.gov
steven.thomas@srs.gov
jennifer.wohlwend@srnl.doe.gov